The Dynamic Amplification Effect of A Site with Earth Fissures: A Case Study in the Taiyuan Basin, China

Jiang Chang
Chang'an University
Yahong Deng (dgdyh@chd.edu.cn)
Chang'an University
Ge Cao
Chang'an University
You Xuan
Chang'an University
Nainan He
Chang'an University
Xunchang Zhao
Chang'an University
Huangdong Mu
Xi'an Technological University

Research Article

Keywords: Dynamic response, Earth fissure, Microtremor, Amplification effect, Seismic fortification

Posted Date: May 19th, 2021

DOI: https://doi.org/10.21203/rs.3.rs-475285/v1

Abstract

As a widespread geological hazard, the disaster development process of earth fissures is irreversible and difficult to control, which seriously affects the construction and safe operation of engineering facilities. However, few clear conclusions and special regulations have been given regarding the influence of earth fissures on the dynamic response characteristics of a site and earthquake prevention and disaster reduction measures. Therefore, the microtremor was used instead of earthquake motions to reveal the dynamic response of a site with fissures. The earth fissures in the Taiyuan Basin, which exhibit a large amount of activity, were used as examples. In order to reveal the dynamic response from several aspects, four methods, including the Fourier spectrum, the horizontal-to-vertical spectral ratio (HVSR), the response acceleration, and the Arias intensity, were employed. The results show that the spectrum peaks increase sharply at an earth fissure and return to a stable value approximately 20–25 m away from the fissure, indicating that the earth fissures have an amplification effect on the dynamic response of the site. Additionally, a greater amplification occurs on the hanging wall of the earth fissure. The influence range of the dynamic response of site can be divided into four areas. Suggestions on the seismic fortification intensity and setback distances were also proposed. The amplification mechanism was summarized as the coupling of the changes in the soil properties caused by earth fissure activity, the catadioptric effect of the earth fissure interface, and the multiple amplifications caused by secondary fissures.

1 Introduction

As a type of geohazard that stretches and ruptures from the shallow rocks to the topsoil, the development of earth fissures is relatively slow, but it is hard to control. Therefore, earth fissures severely restrict any nearby urban land planning and engineering construction projects. From the end of the last century to the beginning of the 21st century, induced by factors, including regional groundwater exploitation caused by global economic development and population expansion, earth fissure disasters have occurred worldwide. A large number of earth fissures have been reported in Iceland (Hauksson 1983), Ethiopia (Ayalew et al. 2004; Williams et al. 2004), Kenya (Ngece and Myambok 2000), Saudi Arabia (Al-Harthi et al. 1999; Youssef and Ahmed 2013), the United States (Neal et al. 1968; Lofgren 1978; Holzer et al. 1979; Jachens et al. 1982), and China (Meyer et al. 1998; Geng and Li 2000; Peng et al. 2007; Deng et al. 2013). The continuous dislocation movement of earth fissures in these areas have caused the differential settlement and tensile fissures on the ground surface. Therefore, there are serious contradictions between earth fissure disasters and road engineering, construction engineering, underground pipeline planning, underground exploitation, and urban construction planning.

In order to reduce the damage earth fissure disasters cause to engineering construction projects, scholars have conducted basic research on the development characteristics, formation mechanism, and activity characteristics of earth fissures (Bouwer 2010; Leonard 1929; Holzer and Gabrysch 2010; Neal et al. 1968; Peng et al. 2016; Deng et al. 2013). Now that the basic information of earth fissures has been determined, it is particularly important to develop disaster prevention and mitigation measures for sites with earth fissures. Since China is the country with the most earth fissures around the world, the contradiction

between urbanization and earth fissure disasters is more salient. In order to solve the earth fissure disaster prevention and mitigation problems, scholars have conducted research on methods of strengthening structures, avoidance distances, and earth fissure activity monitoring (Zhang et al. 2016; Qiao et al. 2018; Zang et al. 2019). However, the dynamic response and earthquake fortification of a site with earth fissures are still unclear.

Earth fissures with a tectonic origin are similar to buried faults in appearance and shape. The amplification effect of the dynamic response of seismogenic faults and non-seismic faults during earthquakes has been confirmed (Marra et al. 2000; Spudich and Olsen 2001), and fortification specifications and standards for many sites with faults have been established (Bouckovalas 2006; Janine et al. 2003; Christenson et al. 2003). Therefore, as a type of surface disaster formed under the effects of a buried fault, regional tectonic stress, and groundwater recession, the dynamic response of a site with earth fissures to earthquakes also deserves attention. Moreover, the seismic response is not the only dynamic problem in sites with earth fissures. Dynamic loads caused by blasting, high-speed ways, and subways can also motivate additional dynamic responses in sites with earth fissures. Therefore, the dynamic response of a site with earth fissures is a particularly important issue for the current pace of urban development. However, previous studies and specifications have only considered the influence range of differential settlement of the ground due to earth fissure activity (Zhang et al. 2006; Lu et al. 2018; Chen 2002). The setback distance of a site with earth fissures based on their dynamic responses requires further study.

Unfortunately, there is an obstacle to studying the dynamic response of a site with fissures. The availability of strong motion data for an earth fissure site is rare, and real-time monitoring while waiting for an earthquake to occur is impractical. Fortunately, the required analysis can be carried out using microtremors, which are readily available. A microtremor signal is a type of stable non-repetitive random wave motion that is excited by natural and artificial random vibration sources. It propagates through the ground while being reflected and refracted multiple times by the strata interfaces. In the 1950s, after conducting a series of studies on microtremors, scholars in Janpan came to the conclusion that the spectral characteristics of microtremors can reflect the dynamic characteristics of engineering sites (Kanai 1954; Aki 1975; Ohta et al. 1978; Kagami et al. 1982, 1986). Since then, through further research, scholars from various countries have continuously improved the technical means of the application of microtremors (Nakamura 1989; Lermo 1994; Field and Jacob 1995; Seekins et al. 1996; Guo et al. 1999).

Therefore, in this study, we used microtremors to analyze the dynamic response of a site with earth fissures. The Fenwei graben in China is one of the regions with the widest, largest, and most active earth fissures in the world. This site contains 107 earth fissures distributed throughout the Taiyuan Basin. The distribution characteristics and activity of the earth fissures in the basin are particularly representative (Peng et al. 2018). Thus, the Fourier spectrum, horizontal-to-vertical spectral ratio (HVSR), response acceleration, and Arias intensity of the microtremors at this site were analyzed using representative earth fissures in the Taiyuan Basin as examples. The spectrum characteristics were clarified, and the amplification effect of the earth fissures on the dynamic response of the site was determined. Finally, in

order to provide suggestions for the seismic fortification of sites with earth fissures, the change in the influence range and the amplification effect were also investigated.

2 Earth Fissures In Taiyuan Basin

2.1 Geologic setting

The Taiyuan Basin is located in the central part of Shanxi Province, and it is a northeast syncline elongated basin under the control of active faults. As can be seen from Fig. 1, the basin is surrounded by Taihang Mountain to the east and Lvliang Mountain to the west, with a total area of about 4000 km^2. This basin is one of the large faulted basins in the Cenozoic faulted belt on the Shanxi continental platform. At the beginning of the Late Tertiary, the north-south regional tectonic stress strengthened, causing the shovel-type faults at the edge of the basin, which were formed by the tectonic activities in the Yanshan Period, to be further developed. The block was depressed along the basin's margin fault, and the Taiyuan Basin began to experience deposition.

The uplift of the upper mantle in the deep part of the basin led to the horizontal flow development of the low velocity, high conductivity layer in the middle crust, which induced the extension of the upper crust and along the fracture surfaces. The resulting shovel-type normal fault at the edge of the basin laid the foundation for the tensile fracturing of the basin structure. Moreover, additional horizontal tensile stress was generated in the shallow surface, which provided a regional tensile environment for the formation of earth fissures. The basement of the Taiyuan Basin undulates, with extensional faults developed and clearly divided fault blocks. The extensional structural characteristics developed under the regional tensile stress provide a convenient environment for the development of earth fissures. The average thickness of the Cenozoic sedimentary layer in the basin is 1000–2000 m, with a maximum thickness of 3800 m. Some of the faults in the Quaternary strata are extensions of basement faults, while others are only developed in the Quaternary soils. These faults are all in a stretched state, indicating that the basin has been in an extensional environment since the Quaternary. These faults of different scales constitute multistage extensional fractures in the Quaternary strata, providing favorable geological conditions for land subsidence. These deep fractures provide the initial fracture source and boundary conditions for the formation of earth fissures. The coverage of the Quaternary strata provides moderately good conditions for the development of earth fissures.

In general, the earth fissures in the Taiyuan Basin formed under the following conditions: an extensional environment for the deep structures, space for the development of deep faults provided by the basement's structure, and a convenient environment for the rupturing the Quaternary sediments. In addition to the geological factors, the over-exploitation of groundwater in the basin has formed a large number of depression cones that have caused regional ground subsidence and eventually induced the widespread development of earth fissures.

2.2 Characteristics of the earth fissures

The earth fissures in the Taiyuan Basin began to emerge on the ground surface in the 1970s. At present, investigations have identified about 107 earth fissures. The earth fissures in this basin are mostly distributed in the piedmont alluvial plains, including the Lvliang piedmont alluvial plain and the Taiyue piedmont alluvial plain. The regional earth fissures in the Taiyuan Basin have the following common characteristics. (1) The trends and occurrences of the fissures are consistent with those of the buried faults. (2) The fissures are mostly concentrated at the edges of the groundwater depression cones. (3) The earth fissures are more densely distributed in the region where the thickness of the Quaternary sediments changes abruptly. According to their distribution, activity characteristics, and formation mechanism, the earth fissures in the Taiyuan Basin can be divided into two regions. Region I is the Qixian-Taigu earth fissure zone, which contains about 51 fissures, and Region II is the Qingxu-Jiangcheng-Wenshui earth fissure zone, which extends for about 46 km (Fig. 2).

2.2.1 Qixian-Taigu earth fissure zone (Region I)

The Qixian-Taigu earth fissure zone is located in the southeastern part of the basin and contains about 51 identified fissures. There are four parallel giant earth fissures in Dongguan Town at the junction of Qixian and Taigu. As shown in Fig. 3, these typical earth fissures (i.e., E1, E2, E3, and E4) are located in DongLZ Village, Baigui Village, Dongguan Substation, and Guanchang Village. The four earth fissures have an overall trend of 65°–75°, and their lengths are all greater than 2 km.

E1 and E4 are 1 km apart, and both extend linearly. The length of their surface outcrops is 22.4 km and 4.45 km, respectively, with widths of 0.3–2 m. The fissures continue to develop at an activity rate of 2–3 cm/a, causing damage to houses and roads. An obvious step with a vertical dislocation of 45 cm can be seen on a road crossed by E1. Fissure E2 crosses Baigui Village with a strike of about 77°. It is inclined at 347° and has a total length of about 6.6 km. This fissure appeared in 1998 and has been continuously active until now. The movement of earth fissures has caused damage to a large number of houses in Baigui Village and has resulted in areas in which the height difference of the ground is 40 cm. E3 is located in the northern part of Dongguan Town, extends for 10.2 km, and has a strike of NE73°. This fissure first appeared in 1978 and became active again after 2000. The activity of this earth fissure has resulted in ground rupture and the formation of dislocation steps on the road.

These four typical earth fissures have the characteristics of vertical differential settlement and lateral horizontal extension. As for their profile characteristics, according to exploratory trench data from previous studies, the activity of the earth fissure increases with depth. The vertical displacement of the earth fissures increases with depth, and they exhibit obvious syn-sedimentary fault structure attributes. Some small secondary fissures have been found in the hanging wall of the earth fissures in Region I. These secondary fissures are mostly within 10 m of the main fissures. They have small widths, small vertical displacements, and barely ruptured the ground surface.

The formation mechanism of the earth fissures in Region I can be summarized as follows. Under the influence of the NW-NNW horizontal tensile stress in the Taiyuan Basin, the hanging wall of the

Hongshan-Fancun fault (F3) has continued to subside. The earth fissures began to grow at depth. After the Tangshan earthquake in 1976, the internal tensile stress of the basin increased rapidly. Under the tensile environment in the basin, the concealed fractures stretched to form rupture deformation that developed from depth toward the surface, forming buried earth fissures below the ground. From the 1980s to the 2000s, due to the over-exploitation of groundwater in the area, the groundwater level dropped significantly. Subsequently, the water-containing layer was densely deformed, and ground subsidence occurred. Under the additional effects of torrential rains and irrigation, the earth fissures reached the surface. The formation mechanism of the earth fissures in Region I can be summarized as the coupling of the creep deformation of buried faults and the over-exploitation of groundwater.

2.2.2 Qingxu-Jiangcheng-Wenshui earth fissure zone (Region II)

The Qingxu-Jiangcheng-Wenshui earth fissure zone is located at the junction of the Jiaocheng uplift and the sedimentary plain. From Qingxu County in the southwest to Wenshui County in the northeast, the earth fissures are intermittently distributed along the trend of the buried Jiaocheng Fault (F1). As shown in Fig. 4, the activity of the earth fissures in this area has caused wall cracks, road damage, and ground fractures. The earth fissures are mostly distributed in areas where the thickness of the Quaternary strata is thinner than 200 m.

According to the investigations in this area, the earth fissures mostly trend NE and are inclined to the SE, with dip angles of 70°–80°. The movement of the earth fissures involves horizontal tension, vertical dislocation, and strike-slip dislocation, which is consistent with the characteristics of the buried faults. The main planar distribution characteristics of the earth fissures include morphological diversity, strike stability, and zonal distribution. According to the profile of the exploratory trench, 2–4 secondary fissures were found on the hanging wall, and 1–2 small secondary fissures were found on the footwall. Under the control of the piedmont faults, the profile morphology of the earth fissures in Region II is mostly steps-type, y-shaped, comb-shaped, and shovel-shaped. As can be seen from Fig. 5, the activities of the main fissures and the secondary fissures have caused the overlying loess layer and the sandy gravel layer to move along the fissures, forming multi-level steep ridges on the surface.

The formation of the earth fissures is mainly controlled by the Jiaocheng Fault, and the enhancement of the neotectonic activity has directly intensified the development of the earth fissures. The NW-SE horizontal tensile tectonic stress in the basin provides a convenient environment for the expansion of the NE-SE trending earth fissures. In the piedmont where region II is located, the ground subsided after the over-pumping of karst groundwater and pore groundwater. As a result, the activity rate of the earth fissures far exceeds that of the buried faults. The formation mechanism of the earth fissures in region II can be summarized as follows: under the control of the buried faults at the basin’s margin, the regional stress provides an environment for fissure propagation, and the over-exploitation of groundwater accelerates the extension of the fissures to the surface.

The distribution characteristics, activity characteristics, and formation mechanism of the earth fissures in the Qixian-Taigu area (Region 1) and the Wenshui-Jiaocheng-Qingxu area are the most representative fissures in the Tiayuan Basin. Therefore, seven microtremor survey lines (L1–L7) were laid over these fissures to analyze the dynamic response of a site containing earth fissures.

3 Methodology

The microtremor signal is a type of stable non-repetitive random wave that propagates through the ground after being repeatedly reflected and refracted by the interfaces of the layers after being excited by natural and artificial random vibration sources. It can be used to determine the dynamic characteristics of the foundation soil of a site. According to the microtremor test research conducted by SEASEM, a microtremor can be regard as the superposition of numerous sin waves with different frequency components (Bard et al. 2008). Therefore, the influence of earth fissures on the dynamic response of a site can be determined based on the frequency spectrum characteristics of the microtremor.

In this paper, a high-sensitivity seismometer with a built in tri-axial velocity meter corresponding to the network (CV-374AV) was used to collect the microtremor at the site with earth fissures. A survey line containing 18 measurement points was laid out perpendicular to an earth fissure in order to compare the variation in the microtremor's characteristics at different distances from the earth fissure. The measurement points close to the earth fissure were arranged more densely. According to the research of SEASEM, the recording time of each point was guaranteed to be greater than 10 min. The time-history velocity curves of the microtremor were obtained in three directions at each point.

Since a microtremor is far less intense than an earthquake's motion, the time-history curves of the measurement points can hardly reflect the variation in the dynamic response. Therefore, a series of frequency domain analyses were performed using the SeismoSignal software. First, the 10 s stationary wave band was cut from the time-history velocity curve and was used to obtain the acceleration curve. After that, the acceleration data were imported into SeismoSignal for Fourier analysis. Since the energy of the earthquake's motion with the most prominent dynamic response is mostly concentrated within 10 Hz, the Butterworth filter was used to perform the 0.1–10 Hz band-pass filtering, followed by a baseline correction (Fig. 6).

In order to reveal the dynamic response of a site containing earth fissures from several aspects, four methods, including Fourier spectrum, HVSR, response acceleration, and Arias intensity, were used. Since the Fourier spectrum and HVSR methods can reflect the inherent dynamic characteristics of the site, the differences in the spectral characteristics of the different measurement points can preliminarily reflect the influence of the earth fissure on the dynamic response. In addition, the differences in the frequency spectrum in the acceleration response spectrum can be used to evaluate the dynamic response characteristics of a structure in a site containing earth fissures. Moreover, the Arias intensity can also reflect the accumulation of microtremor energy during the interception period to further demonstrate the dynamic response of a site containing earth fissures.

4 Result

4.1 Frequency content

The investigations revealed that the scale, formation mechanism, and the development characteristics of the earth fissures in the two regions are different. The earth fissures in Region I were formed by the coupling of the creep deformation of the buried faults and the over-exploitation of groundwater. The number of secondary fissures around the main fissures in this area is small, and the activity is also small. The large-scale earth fissure groups in Region II were formed under the control of the buried fault on the basin's margin, the regional stress provides the environment for fissure expansion, and the over-exploitation of groundwater accelerates the expansion process. The secondary fissures distributed in the steps on both sides of the main fissure have ruptured the surface, forming dislocation steps. Region I can be regarded as a site with only a single fissure, while region II can be regarded as a site with a main fissure and secondary fissures. After processing the microtremor data, it was found that the spectral characteristics of the earth fissures in the same region are similar. Therefore, taking survey L1 in Baigui Village (Region I) and survey line L5 in Wenshui (Region II) as representative lines in the two regions, the spectrum frequency contents of the sites with earth fissures were described in detail as follows.

1. Region I (L2 in Baigui)

As shown in Fig. 7a, the direct Fourier spectrum and HVSR, which reflect the inherent information of the site, have the following characteristics. (1) The dominant frequency peaks of the Fourier spectrum of the measurement points within 10 m on both sides of the fissure are significantly prominent. The average predominant frequency in each direction is 2–4 Hz. (2) The spectrum curves at the measurement points far away from the earth fissure are relatively smooth, and the spectrum peaks are not very prominent. That is, the microtremor propagation at the measurement points 20 m away from the earth fissure is hardly affected by the earth fissure. (3) The horizontal and vertical Fourier spectrum peaks rise rapidly at the earth fissure and gradually attenuate about 20–25 m from the fissure. (4) A greater amplification effect occurs on the hanging wall of the earth fissure. The peak value of the Fourier spectrum within 3 m of the hanging wall of the fissure is significantly larger than that of the footwall. Moreover, the attenuation speed of the peak value of the measurement points on the hanging wall is also lower than those on the footwall.

In order to determine the dynamic response characteristics of the structures in the site containing earth fissures, the acceleration response spectrum was used to reflect the variation in the acceleration response of the single particle system with a natural particle vibration period. The response acceleration is shown in Fig. 7b. (1) The bandwidth of the response acceleration spectrum is narrow, and the peak form is mainly a single peak. (2) At measurement points A1, A2, B1, and B2, which are within 3 m of the earth fissure, the spectrum's peaks are more prominent. (3) The response acceleration peak attenuates as it moves away from the earth fissure, and it remains stable beyond 15–20 m. (4) The peak value on the

hanging wall is slightly larger than that on the footwall. The dynamic response of the site with normal-type earth fissures is greater on the hanging wall.

The Arias intensity reflects the variation characteristics of the microtremor accumulated over time, thereby the dynamic response of the different positions can be determined. The Arias intensity curves of the 18 measurement points on both sides of the earth fissure (Fig. 7c) have the following characteristics. (1) The intensity of the microtremor continues to increase over time until it reaches its maximum value. Moreover, the Arias intensity increases faster, and the peak value is higher near the earth fissure. (2) A greater amplification also occurs on the hanging wall of the earth fissure. (3) The intensity curves of the points that are 20 m away from the earth fissure are relatively smooth. The intensity peaks at these points are low and are basically the same, which can be regarded as the original intensity of the site when it was barely affected by earth fissures.

2. Region II (L5 in Wenshui)

As shown in Fig. 8, the Fourier spectrum and HVSR of survey line L5 in Region II have the following characteristics. (1) The peaks of the spectrum are sharp, narrow, and multimodal, with three or more secondary peaks near the main peak. The occurrence of multiple secondary peaks is due to the large number of sand and gravel layers in the shallow surface. (2) The predominant frequency of this site is about 2.9–4.1 Hz. There is no obvious relationship between the predominant frequency and the distance from the earth fissure. (3) The spectrum peaks of the measurement points near the earth fissure are sharper and more prominent than those far from the earth fissure, especially at A1–A3 and B1–B3. The spectrum peak gradually decays to a low and stable value with distance from earth fissure. (4) The spectrum peaks of the measurement points on the hanging wall (especially at A1 and A2) are higher than those on the footwall, indicating the greater amplification effect of the hanging wall.

As can be seen from Fig. 8b, the response acceleration curves are mostly multimodal. The amplification effect can also be seen near the earth fissure. The Arias intensity curves are shown in Fig. 8c. The intensity of the microtremor increases with time. Moreover, the increases in the velocity and peak value of the intensity near the earth fissure are higher. While the intensity 20–25 m away from earth fissure is low and hardly changes.

In addition to the previously mentioned lines L2 and L5, the spectrum content of each survey line in the Taiyuan Basin is slightly different. As the ground conditions change, the frequency content, which reflects the inherent conditions of the site, changes, including the peak type, predominant frequency, and bandwidth. However, a similar amplification effect occurred for seven of the survey lines. The amplification effect of the earth fissure on the dynamic response of the site is significantly obvious in the Fourier spectrum, HVSR, response acceleration, and Arias intensity. However, the amplitudes of the four methods have different meanings, and the magnitudes of their peaks are also different for the different

sites. Therefore, the ratio of the affected peak value to the unaffected peak is used as a unified scale for determining the amplification effect.

4.2 Amplification effect

The spectrum contents of the representative earth fissures in the Taiyuan Basin show that the existence of earth fissures amplifies the dynamic response of the site. The results show that the spectrum peaks attenuate to a stable value about 25 m away from the fissure. Therefore, these peak values can be regarded as the original value of the site, i.e., when it was not affected by the earth fissures. The amplification factor of the earth fissure on the dynamic response of the site is defined as the ratio of the spectral peak value of each point to the unaffected peak value. In this way, the amplification effects in different regions, due to different earth fissures, and observed using different spectra can be compared intuitively. Figure 9 shows the amplification factors of seven representative earth fissures obtained using four methods.

As can be seen from the curves, the amplification factors are higher near the fissure. As the distance from the earth fissure increases, the factors attenuate and stabilize at 20–25 m from the earth fissure. By comparing the amplification factor curves of the hanging wall and the footwall of an earth fissure, it was found that a greater amplification occurs in the hanging wall. The amplification factor of a measurement point 3–5 m from the fissure on the hanging wall is consistent with that of a measurement point close to the fissure on the footwall. Although a common amplification effect was observed for the sites containing earth fissures in the Taiyuan Basin, the magnification and the attenuation process of the factors are slightly different.

Survey lines L1–L4 were located in the Qixian-Taigu earth fissure zone (Region I). The earth fissures in this area are mostly single fissures with small, shallow secondary fissures. Because they are only affected by a single earth fissure, the amplification factor curves of lines L1–L4 decay smoothly and quickly. They attenuate to 1 at about 16–20 m from the earth fissure on the hanging wall and attenuate to 1 less than 16 m from the earth fissure on the footwall. As shown in Fig. 9, the shapes of the amplification curves of survey lines L5–L7 in Region II are different from those in Region I.

This investigation has shown that there are very active secondary fissures on both sides of the main fissures in Region II. These secondary fissures have large dislocations and have ruptured the ground surface. Affected by these secondary fissures, amplification factor is slightly higher at 15 m from the fissure on the hanging wall for line L5, 20 m on the hanging wall for line L6, and 8 m on the footwall for line L7. After this, the amplification factor starts to decay again and forms a larger amplification range. Unlike in Region I, the amplification factor of line L5 for an earth fissure in Wenshui attenuates to 1 at about 20 m from the fissure on the hanging wall. However, the attenuation is relatively faster on the footwall, approaching 1 at about 8–16 m from the fissure. The secondary fissure located 20 m from the main fissure on the hanging wall of the earth fissure in Jiaocheng leads to a slower attenuation of the amplification factor for line L6. After a small increase at 20 m, the amplification factor decreases again and approaches 1 at about 25 m from the fissure. It becomes almost stable before 20 m from the earth

fissure on the footwall. The secondary fissure on the footwall of the Qingxu fissure slows down the attenuation process of the amplification effect for line L7. Therefore, the amplification effect on the hanging wall and footwall of the Qingxu earth fissure is similar, becoming stable at about 24 m from the fissure.

By analyzing the amplification factors of the representative earth fissures in the Taiyuan Basin, it was found that an earth fissure will stimulate the amplification effect of the dynamic response of the site. The amplification will attenuate with increasing distance from the fissure. Moreover, the amplification effect is more prominent in the hanging wall. In order to reveal the influence range of the amplification and the seismic fortification distance, the amplification factors of the representative earth fissures in the basin were fitted.

4.3 Seismic fortification distance

The influence range of the earth fissures on the dynamic response of the site was determined by concatenated exponential fitting of the seven amplification factor curves. The fitting curve of the Fourier spectrum amplification factor is shown in Fig. 10a. The dynamic response was amplified twice within 5 m on the hanging wall and decayed to 1.5 times at about 9 m from the fissure. Eventually, it decreased to 1 at about 24 m from the fissure. The amplification factor of the earth fissure was greater than 1.5 within 4 m, and it decayed to a safe value about 20 m away from the fissure. The fitting curve of the response acceleration amplification factor is shown in Fig. 10b. The amplification factor was greater than 2 within 6 m on the hanging wall and within 4 m on the footwall, making this the high-risk zone. The amplification effect decreased to 1.5 times between 6 and 10 m on the hanging wall and 4 and 8 m on the footwall, making this the medium-risk zone. The low-risk zone is 10–20 m from the fissure on the hanging wall and 8–16 m on the footwall. In the low-risk zone, the amplification effect dies down. However, the area more than 20 m from the fissure on the hanging wall and 16 m on the footwall is the safe original site, which is not affected by the earth fissure. The amplification factor of the Arias intensity curve reveals that the amplification is greater than 2 within 9 m of the fissure on the hanging wall. Then, it decreased to 1.5 times at about 15 m and attenuated to the original value after 24 m. As for the footwall, the high-risk zone with twice the magnification is within 6 m of the fissure. The medium-risk zone with 1.5 times the magnification is 6–10 m from the fissure. The change in the attenuation of the amplification factor determined using the HVSR method is shown in Fig. 10d. The amplification effect on the hanging wall of the earth fissure is greater than 2 within 9 m of the fissure, but it decreases rapidly to 1.5 times within 9–15 m. It is magnified by 2 within 6 m on the footwall and attenuates to 1.5 times after 10 m. The area beyond 26 m from the fissure on the hanging wall and 24 m on the footwall is the safe area without amplification.

The distances of the different amplification factors of the earth fissures in the Taiyuan Basin are presented in Table 1. The average high-risk distance is 7.3 m on the hanging wall and only 4 m on the footwall. Since the dynamic response in this range is amplified by more than 2 times, it is not recommended that any construction projects be undertaken in this area. The range in which the dynamic response amplification is 1.5–2 times is the medium-risk zone. Therefore, within 12.3 m on the hanging

wall and 8 m on the footwall, only temporary buildings of low importance, with a short service life, and low seismic fortification requirements should be constructed. Further than 23.5 m from the fissure on the hanging wall and 20 m on the footwall is the low-risk area with only a slight amplification effect. Buildings can be arranged appropriately in this area, but the seismic fortification intensity of the proposed buildings should be increased to 1.5 times the designed value. When some parts of the structure or infrastructure of the building are located within the medium-risk zone, the fortification intensity of the overall structure should also be increased to at least twice that of the original design to ensure safety. In the area beyond 23.5 m from the fissure on the hanging wall and 20 m on the footwall, there is no need to consider the amplification effect of the dynamic response.

Table 1
Recommended seismic fortification distance

Amplification factor	Hanging wall			Footwall		
	1	1.5	2	1	1.5	2
Fourier amplitude	24.0 m	9.0 m	5.0 m	20.0 m	4.0 m	-
Response acceleration	20.0 m	10.0 m	6.0 m	16.0 m	8.0 m	4.0 m
Arias intensity	24.0 m	15.0 m	9.0m	20.0 m	10.0 m	6.0 m
HVSR	26.0 m	15.0 m	9.0 m	24.0 m	10.0 m	6.0 m
Average	23.5 m	12.3 m	7.3 m	20.0 m	8.0 m	4.0 m

Since the earth fissures in the Taiyuan Basin are mostly distributed in the piedmont on the edge of the basin and within the sedimentary areas inside the basin, the distribution characteristics, formation mechanism, and activity characteristics of earth fissures in the two regions are different. Therefore, the amplification effects of the earth fissures in the different regions were compared. The differences in the amplification factors in two regions are shown in Fig. 11. Since there are more secondary fissures in the piedmont area of Region II, and the activity of these fissures is greater, the range of each risk area is wider than that in Region I. Therefore, the seismic fortification intensity of a site with earth fissures in the piedmont area requires additional safety measures.

5 Discussion Of The Amplification Mechanism

This article have revealed the amplification of the dynamic response of sites with earth fissures using microtremors. The mechanism of amplification mostly depends on the soil around the earth fissure and the earth fissure itself.

1. The activity of earth fissures changes the properties of the shallow surface soil. At present, earth fissures are mostly formed under the control of buried faults and due to the over exploitation of groundwater in the area. The activity of these earth fissures increases sharply as the groundwater table decreases and due to the infiltration of surface water from heavy rains, which results in large

vertical dislocations and horizontal extensions. These movements cause the soil on both sides of the earth fissure to become looser. In addition, the surface water infiltration and the refilling of the earth fissures exacerbate this phenomenon. According to the conservation of elastic wave energy (energy flux = $\rho v_s u^2$), for soil layers with the same energy flux, the density is lower near the fissure, and the shear wave velocity of loose soil is lower, so the particle velocity, u, must increase. Therefore, the dynamic response is amplified near the earth fissure. Additionally, since the settlement displacement on the hanging wall of a normal-type fissure causes the soil to become looser, the amplification effect is greater on the hanging wall.

2. Since an earth fissure can be regard as the interface during propagation, the amplification of the dynamic response of the site is manifested in two aspects: refraction and reflection. According to Snell's law, when the incidence angle is greater than a certain critical angle, the generated transmitted wave will slide along the interface. As there are earth fissures in the site, the weak zone formed by the rupture and tension of the earth fissure can be regarded as the propagation interface. This interface provides a convenient channel for the generation of sliding waves and increases the dynamic response near the earth fissure. Moreover, when the earth fissure becomes the propagation interface, dynamic loads including microtremors, ground motions, nearby stable dynamic loads, and other random impacts will be reflected at various angles. Unlike a site without earth fissures, this reflection will cause part of the vibration to be blocked and reflected into the ground, thereby forming an amplification effect near the fissure. Since the normal-type earth fissure dips toward the hanging side, it is more conductive to the reflection of various vibration waves toward the earth fissure, creating a greater amplification in the hanging wall.
3. When there are secondary fissures with obvious dislocations near the main fissure, the amplification created by the main fissure will be increased again by the secondary fissures. The multiple reflections between the main fissure and the secondary fissures lead to a more significant amplification and a larger influence range.
4. In addition, under the action of strong vibrations, the friction and collision of the soil on both sides of the earth fissure also stimulate a further dynamic response. In most sites with earth fissures, the most common way to deal with the differential settlement of the hanging wall of the earth fissure is to backfill and compact the area. However, due to the continuous activity of earth fissures, this part of the overlying backfilled soil easily becomes loose or even separates from the lower part. When a strong vibration strikes, the friction and collision between the loose or separated soil in the hanging wall and the original soil in the footwall will cause a strong dynamic response, resulting in a serious seismic hazard.

6 Conclusions

Using microtremor tests combined with the Fourier spectrum, response acceleration, Arias intensity, and HVSR, methods, in this study, we analyzed the spectral characteristics of sites containing representative earth fissures in the Taiyuan Basin. The amplification effect of the earth fissure on the dynamic response of the site was determined based on the attenuation of the spectral peaks. The results show that there are

certain differences in the spectral characteristics of the seven survey lines in the two regions. The predominant frequencies, peak shapes, bandwidths, and number of peaks are different. However, the peaks obtained using the Fourier spectrum, response acceleration, Arias intensity, and HVSR methods are significantly larger near the fissure and attenuate with increasing distance from the earth fissure. Moreover, a greater amplification effect was observed on the hanging wall of normal-type earth fissures.

In order to provide specific suggestions for the seismic fortification of similar earth fissure sites, the ratio of the peak value of the measurement points to the original peak value of the site was defined as the amplification factor to intuitively measure the amplification effect. The results show that on the hanging wall of the earth fissure, 0–7.3 m from the fissure is the high-risk area, 7.3–12.3 m is the medium-risk area, and 12.3–23.5 m is the low-risk area. However, the influence range on the footwall is lower, with the high-risk area being within 4 m of the fissure, the medium-risk area being 4–8 m from the fissure, and the low-risk area being 8–20 m from the fissure. The safe zone is more than 23.5 m away from the earth fissure on the hanging wall and only 20 m on the footwall. Since the dynamic response in the high-risk zone is amplified by more than 2 times, it is recommended that buildings not be constructed in this zone. The seismic fortification intensity of the structures in the medium-risk zone should be doubled to ensure safety. The seismic fortification intensity of the low-risk zone should be increased to 1.5 times, while the safe area is not affected by the amplification effect of the earth fissure on the dynamic response of the site. In addition to the average fortification distance of a site with earth fissures, this study also analyzed the differences in the amplification effect of the earth fissures on the dynamic response of a site in two regions. A smaller influence range was determined for the Qixian-Taigu earth fissure zone (Region I). Due to the secondary fissures near the main fissures in the Jiaocheng earth fissure zone (Region II), a larger amplification of the dynamic response occurred in the site with secondary earth fissures.

Finally, the mechanism of the dynamic response amplification of the site with earth fissures was also investigated. The changes in the soil properties caused by earth fissure activity and the catadioptric effect of the earth fissure interface result in the amplification effect. Based on the variation in the microtremor spectral peaks, the amplification effect of the earth fissures on the dynamic response of the site was determined. Preliminary suggestions for seismic fortification were also given. In order to provide the most practical suggestions for engineering construction projects, it is necessary to further analyze the dynamic response characteristics of different types of structures in sites with earth fissures.

7 Declarations

We declare that we do not have any commercial or associative interest that represents a conflict of interest in connection with the work submitted. The data sets supporting the results of this article are included within the article and its additional files. All authors have read and approved this version of the article, and due care has been taken to ensure the integrity of the work. Neither the entire paper nor any part of its content has been published or has been accepted elsewhere. It is not being submitted to any other journal.

Acknowledgments

This research was supported by the National Natural Science Foundation of China (Grant No. 41772275) and the Fundamental Research Funds for the Central Universities (No. 300102268203, No. 300102261716). All of the support provided is gratefully acknowledged.

8 References

1. Al-Harthi AA, Bankher KA (1999) Collapsing loess-like soil in western Saudi Arabia. J Arid Environ 41:383–399
2. Aki K (1957) Space and time spectra of stationary stochastic waves, with special reference to microtremors. Bull Earthq Res Inst 35:415–456
3. Ayalew L, Yamagishi H, Reik G (2004) Ground cracks in Ethiopian Rift Valley: facts and uncertainties. Eng Geol 75:309–324
4. Bard PY, Acerra C, Aguacil G et al (2008) Guidelines for the Implementation of the H / V Spectral Ratio Technique on Ambient Vibrations Measurements, Processing and Interpretation. Bull Earthq Eng 6(4):1–2
5. Bouckovalas G (2006) ETC-12: Geothchnical Evaluation and Application of the Seismic Eurocode EC8. National Technical University, Greece, pp 55–64
6. Bouwer H (2010) Land Subsidence and Cracking Due to Ground-Water Depletiona. GROUNDWATER 15:358–364
7. Chen ZX (2002) Mechanism of ground fissure and its prevention countermeasures. Journal of Xi`an Engineering University 24(2):17–20. (In Chinese with English abstract)
8. Christenson Gary E, Darlene Batatian L, Nelson Craig V (2003) Guidelines for Evaluating Surface-Fault-Rupture in Utah. Geological Survey, Utah, pp 5–23
9. Deng YH, Peng JB, Mu HD, Li L, Sun Z (2013) Ground Fissures Germination Mechanism of Deep Structure Activities in Weihe Basin. J Jilin Univ 43(2):521–527
10. Field EH, Jacob KH (1995) A comparison and test of various site-response estimation techniques, including three that are not reference-site dependent. B Seismol Soc Am 85:1127–1143
11. Geng DY, Li ZS (2000) Ground fissure hazards in the USA and China. Earthquake Science 13(04):466–476
12. Guo M, Xie L, Gao E, Liu C (1999) Review for analysis of site response by microtremors. World information on earthquake engineering 3:14–19
13. Hauksson E (1983) Episodic rifting and volcanism at Krafla in north Iceland- growth of large ground fissures along the plate boundary. J Geophys Res Solid Earth 88(B1):625–636
14. Holzer TL, Pampeyan EH (1979) Earth fissures and localized differential subsidence. Water Resour Res 17:223–227

15. Holzer TL, Gabrysch RK (2010) Effect of Water-Level Recoveries on Fault Creep. Houston Texas GROUNDWATER 25:392–397
16. Lermo J FC (1994) Are microtremors useful in site response evaluation? B Seismol Soc Am 84:1350–1364
17. Jachens RC, Holzer TL (1982) Differential compaction mechanism for earth fissures near Casa Grande, Arizona. Geol Soc Am Bull 93(10):998–1012
18. Janine Kerr S, Nathan R, Van Dissen et al (2003) Planning for Development of Land on or Close to Active Faults. Wellington: Institute of Geological & Nuclear Science Client Report 2–50
19. Kagami H, Duke CM, Liang GC, Ohta Y (1982) Observation of 1-to 5-second microtremors and their application to earthquake engineering. Part II. Evaluation of site effect upon seismic wave amplification due to extremely deep soil deposits. B Seismol Soc Am 72:987–998
20. Kagami H, Okada S, Shiono K, Oner M, Dravinski M, Mal AK (1986) Observation of 1-to 5-second microtremors and their application to earthquake engineering. Part III. A two-dimensional study of site effects in the San FernandoValley. B Seismol Soc Am 76:1801–1812
21. Kanai K (1954) Measurement of microtremor. I Res. Inst. 199–209
22. Leonard RJ (1929) An Earth Fissure in Southern Arizona. J Geol 37:765–774
23. Lofgren BE (1978) Hydraulic stresses cause ground movement and fissures, Picacho, Arizona. Geological Society American Abstracts Programs 10:113
24. Lu QZ, Peng JB, Deng YH et al (2014) Failure characteristics and influence width of Beiqijia-Gaoliying ground fissure in Beijing. Geotechnical Investigation Surveying 42(06):5–11. (In Chinese with English abstract)
25. Marra F, Azzara R, Bellucci F et al (2000) Large amplification of ground motion at rock sites within a fault zone in Nocera Umbra (central Italy). J SEISMOL 4:543–554
26. Meyer B, Tapponnier P, Bourjot L et al (1998) Crustal thickening in Gansu-Qinghai, lithospheric mantle subduction, and oblique, strike-slip controlled growth of the Tibet plateau. Geophys J Int 135(1):1–47
27. Nakamura Y (1989) A method for dynamic characteristics estimation of subsurface using microtremor on the ground surface. Railway Technical Research Institute Quarterly Reports 30
28. Neal JT, Langer AM, Kerr PF, Paul F (1968) Giant Desiccation Polygons of Great Basin Playas. Geol Soc Am Bull 79(1):69
29. Ngece WM, Myambok IO (2000) Ground subsidence and its socio-economic implications on the population: a case study of the Nakuru area in Central Rift Valley. Kenya Environmental Geology 39(6):567–574
30. Ohta Y, Kagami H, Goto N, Kudo K (1978) Observation of 1-to 5-second microtremors and their application to earthquake engineering. Part I: Comparison with long-period accelerations at the Tokachi-Oki earthquake of 1968. B Seismol Soc Am 68:767–779
31. Peng JB, Li XA, Fan W (2007) Classification and development pattern of caves in the loess plateau. Earth Sci Front 14(6):234–244

32. Peng JB, Qiao JW, Leng YQ et al (2016) Distribution and mechanism of the ground fissures in Wei River Basin, the origin of the Silk Road. Environ Earth Sci 75(8):718
33. Peng JB, Meng LC, Lu QZ et al (2018) Development characteristics and mechanisms of the Taigu-Qixian earth fissure group in the Taiyuan basin, China. Environ Earth Sci 77(11):407
34. Qiao JW, Peng JB, Deng YH et al (2018) Earth fissures in Qinglong Graben in Yuncheng Basin, China. J Earth Syst Sci 127(1):10
35. Seekins LC, Wennerberg L, Margheriti L, Liu HP (1996) Site Amplification at Five Locations in San Francisco, California: A Comparison of S Waves, Codas, and Microtremors. Bullseismsocam 86:627–635
36. Spudich P, Olsen KB (2001) Fault zone amplified waves as a possible seismic hazard along the Calaveras fault in central California. GEOPHYS RES LETT 28:2533–2536
37. Williams FM, Williams MAJ, Aumento F (2004) Tensional fissures and crustal extension rates in the northern part of the Main Ethiopian Rift. Journal of African Earth Science 38(2):183–197
38. Youssef AM, Maerz NH (2013) Overview of some geological hazards in the Saudi Arabia. Environmental Earth Science 70(7):3115–3130
39. Zang MD, Peng JB, Qi SW (2019) Earth fissures developed within collapsible loess area caused by groundwater uplift in Weihe watershed, northwestern China. J Asian Earth Sci 173:364–373
40. Zhang SM, Zhang JM et al (2006) DBJ 61-6-2006, Specification for Site Investigation and Engineering Design on Xi'an Ground Fractures. Xi`an: Shaanxi Province construction standard design station 6–7. (Specification In Chinese)
41. Zhang Y, Wang Z, Xue Y et al (2016) Mechanisms for earth fissure formation due to groundwater extraction in the Su-Xi-Chang area, China. Bull Eng Geol Env 75(2):745–760

Figures

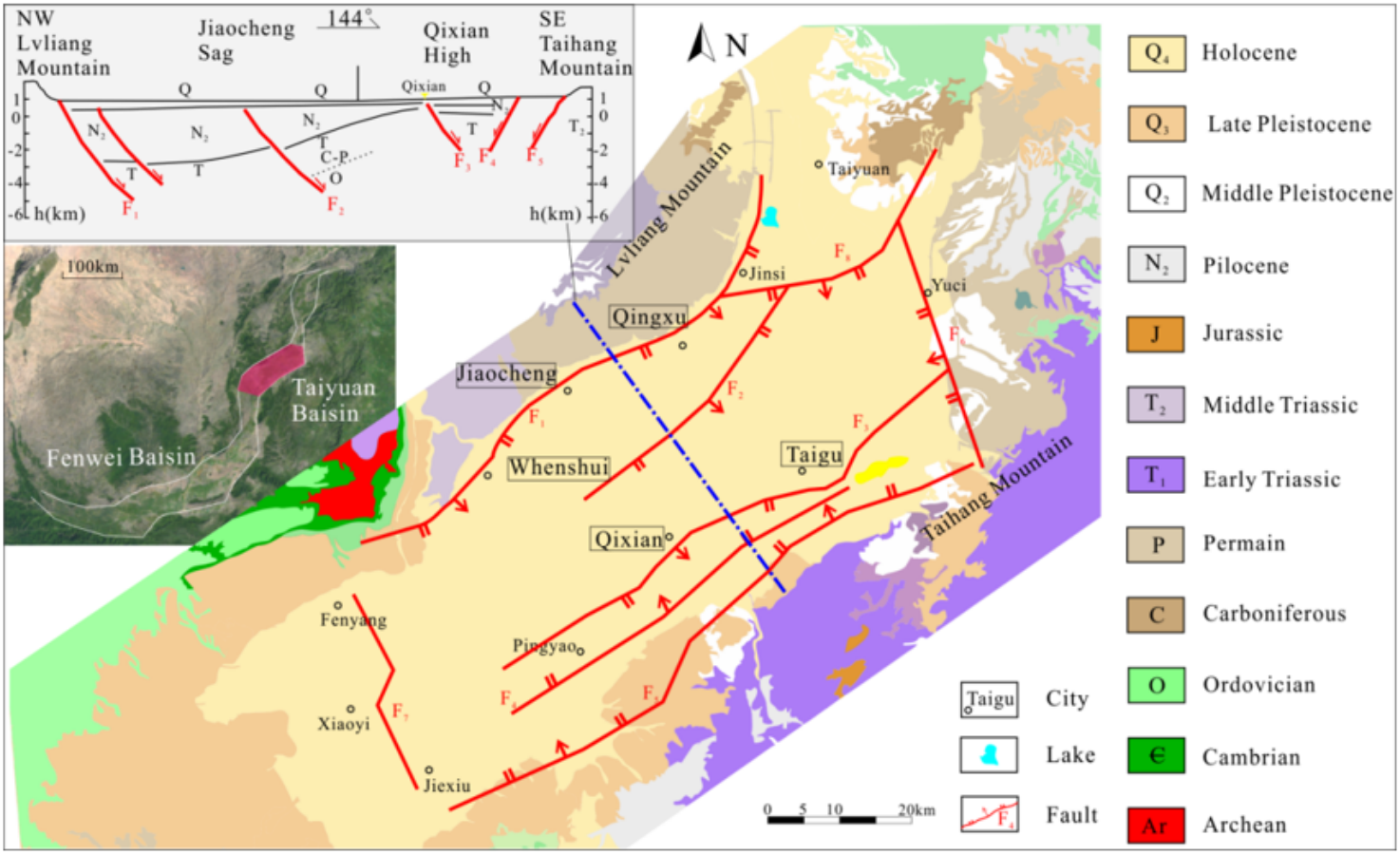

Figure 1

Regional structure of the Taiyuan Basin Note: The designations employed and the presentation of the material on this map do not imply the expression of any opinion whatsoever on the part of Research Square concerning the legal status of any country, territory, city or area or of its authorities, or concerning the delimitation of its frontiers or boundaries. This map has been provided by the authors.

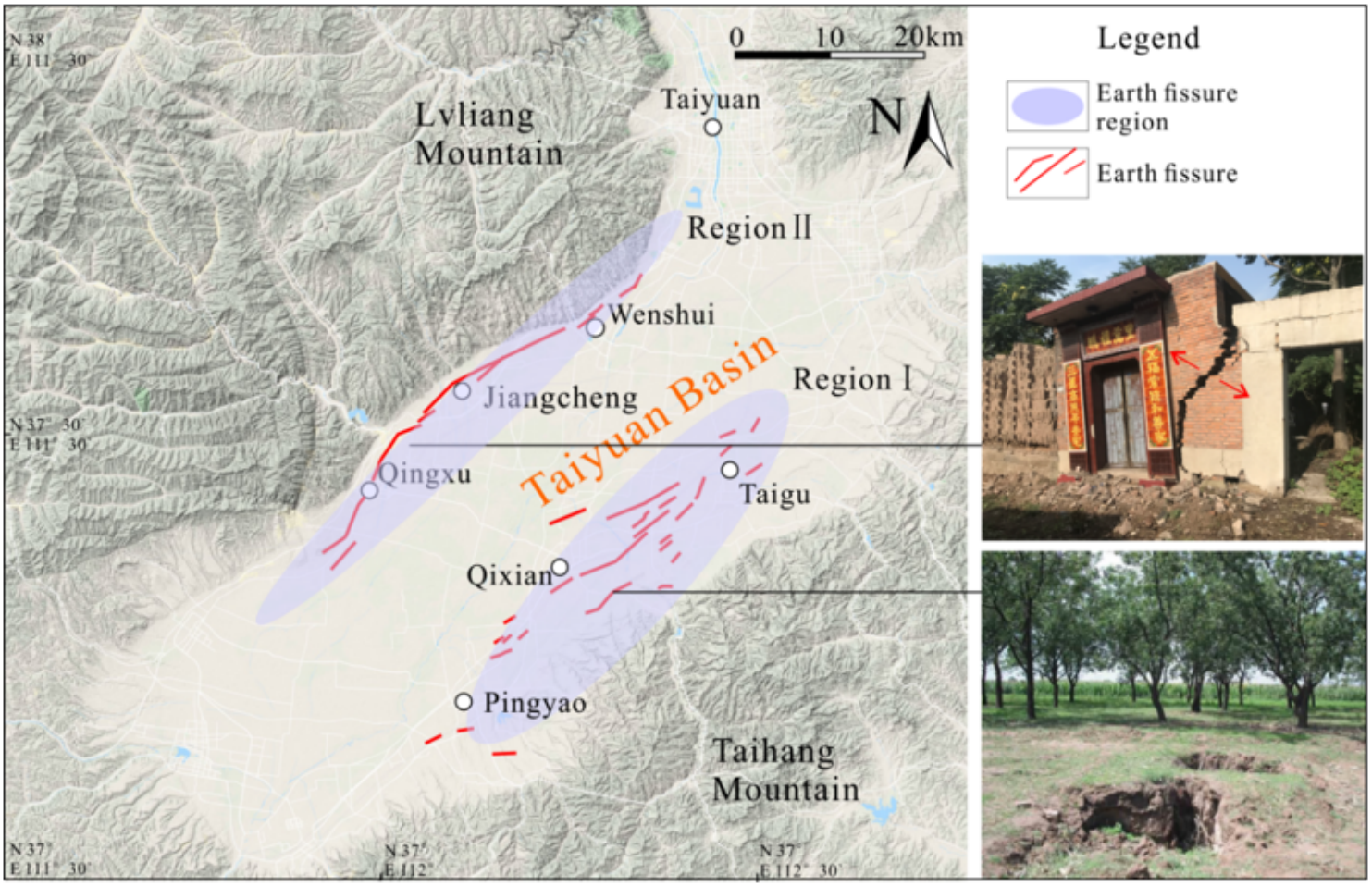

Figure 2

Distribution of the earth fissures in the Taiyuan Basin Note: The designations employed and the presentation of the material on this map do not imply the expression of any opinion whatsoever on the part of Research Square concerning the legal status of any country, territory, city or area or of its authorities, or concerning the delimitation of its frontiers or boundaries. This map has been provided by the authors.

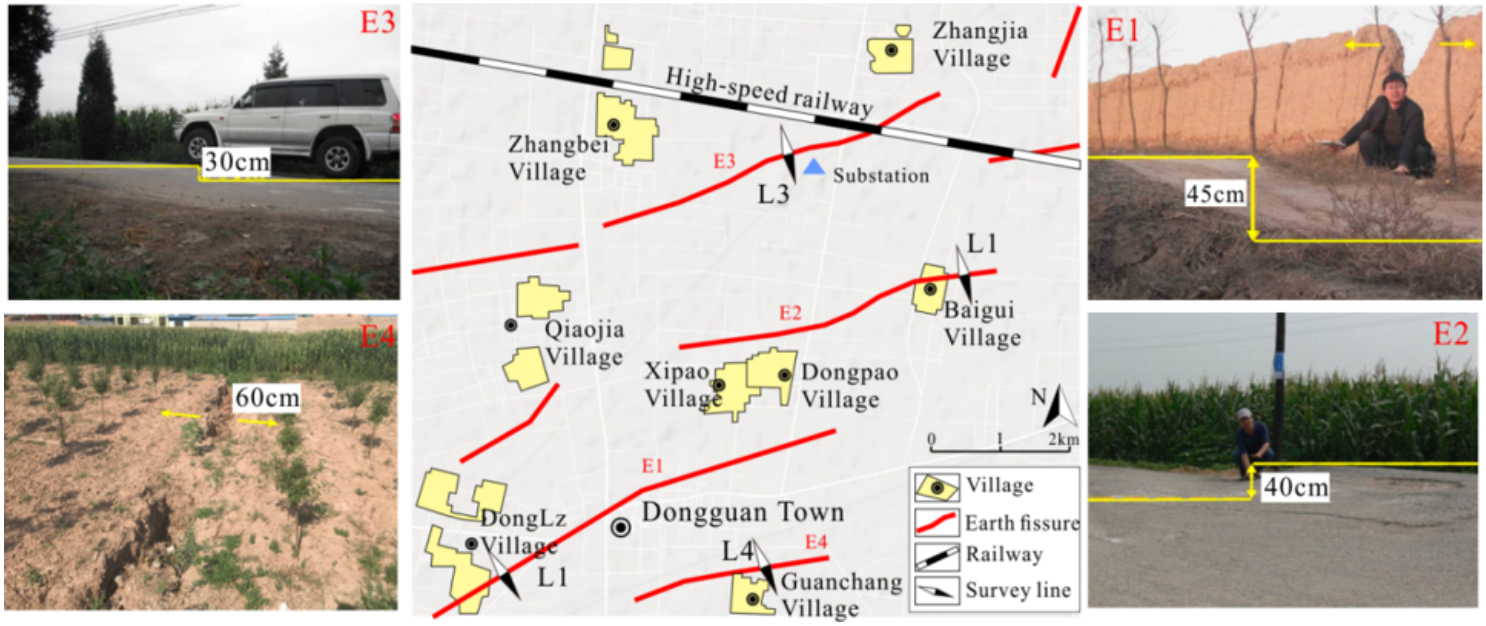

Figure 3

Distribution of typical earth fissures in the Qixian-Taigu area (Region I) Note: The designations employed and the presentation of the material on this map do not imply the expression of any opinion whatsoever on the part of Research Square concerning the legal status of any country, territory, city or area or of its authorities, or concerning the delimitation of its frontiers or boundaries. This map has been provided by the authors.

Figure 4

Earth fissure disasters in Region II (Qingxu-Jiacheng-Wenhui)

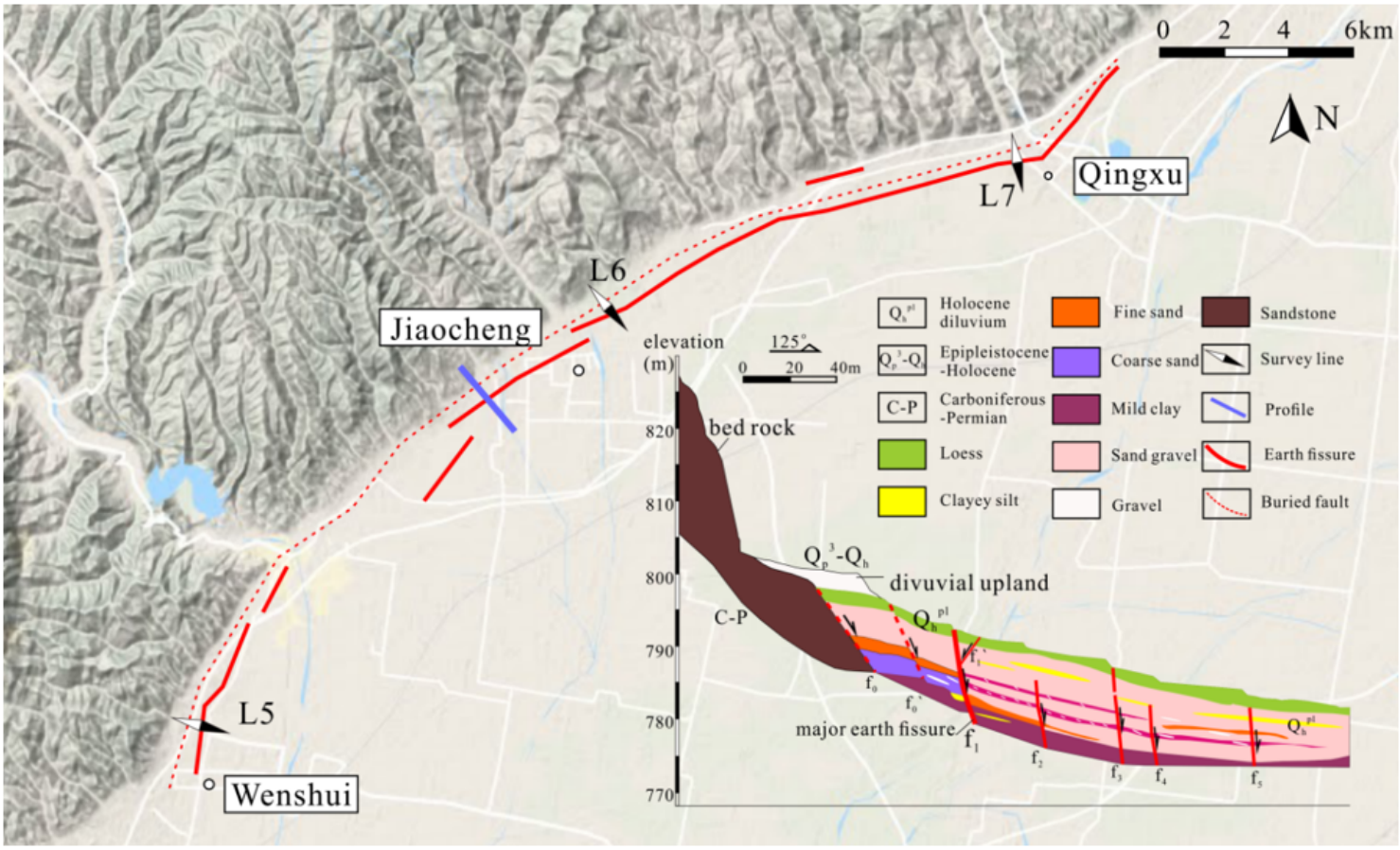

Figure 5

Earth fissures in Region II Note: The designations employed and the presentation of the material on this map do not imply the expression of any opinion whatsoever on the part of Research Square concerning the legal status of any country, territory, city or area or of its authorities, or concerning the delimitation of its frontiers or boundaries. This map has been provided by the authors.

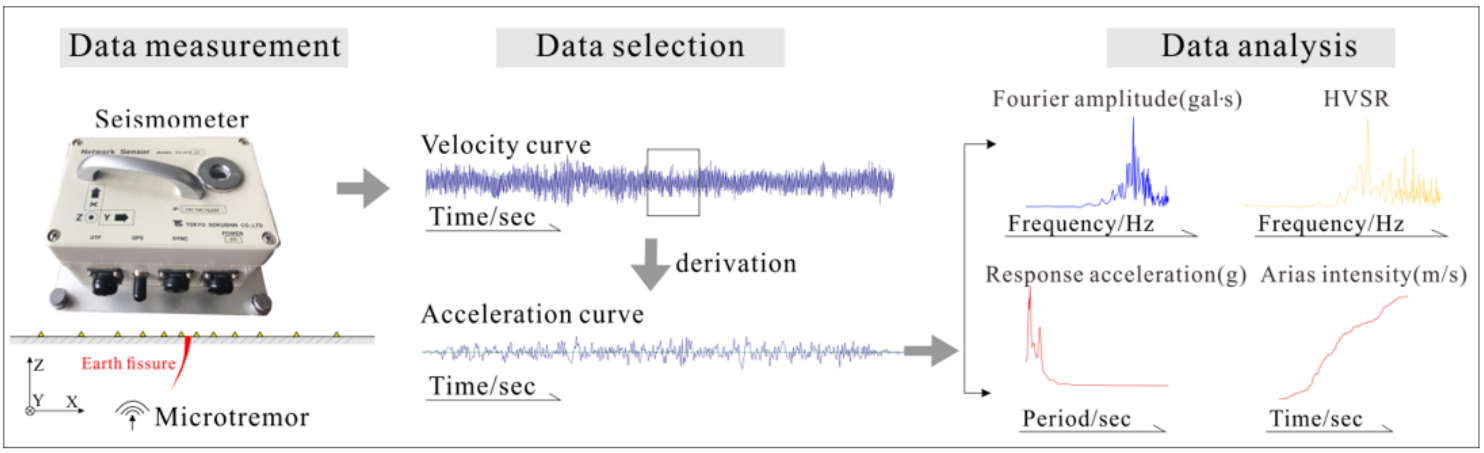

Figure 6

The data processing of the microtremor

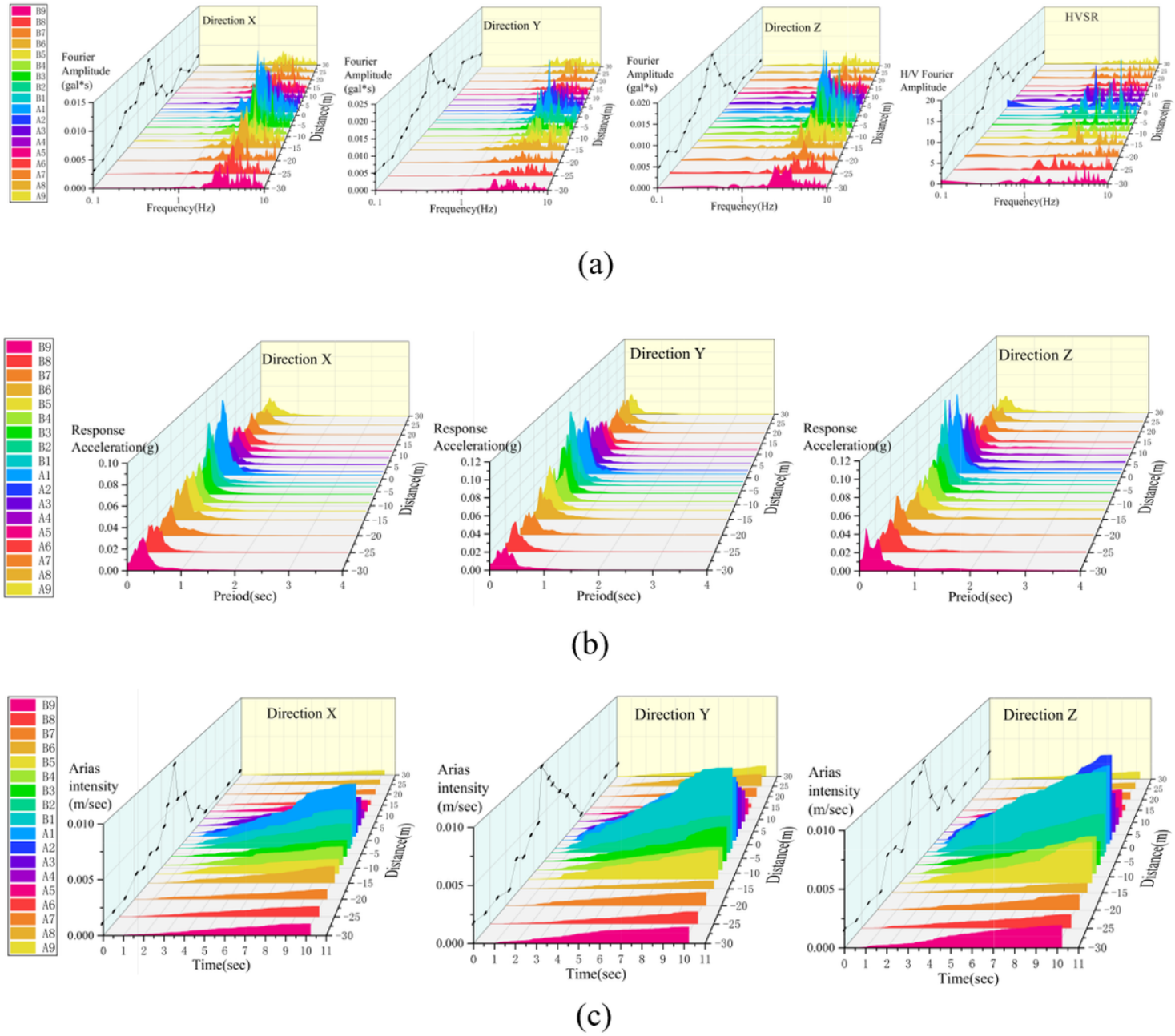

Figure 7

The frequency content of line L2 in Baigui. a) Fourier amplitude and HVSR, b) Response acceleration, and c) Arias intensity.

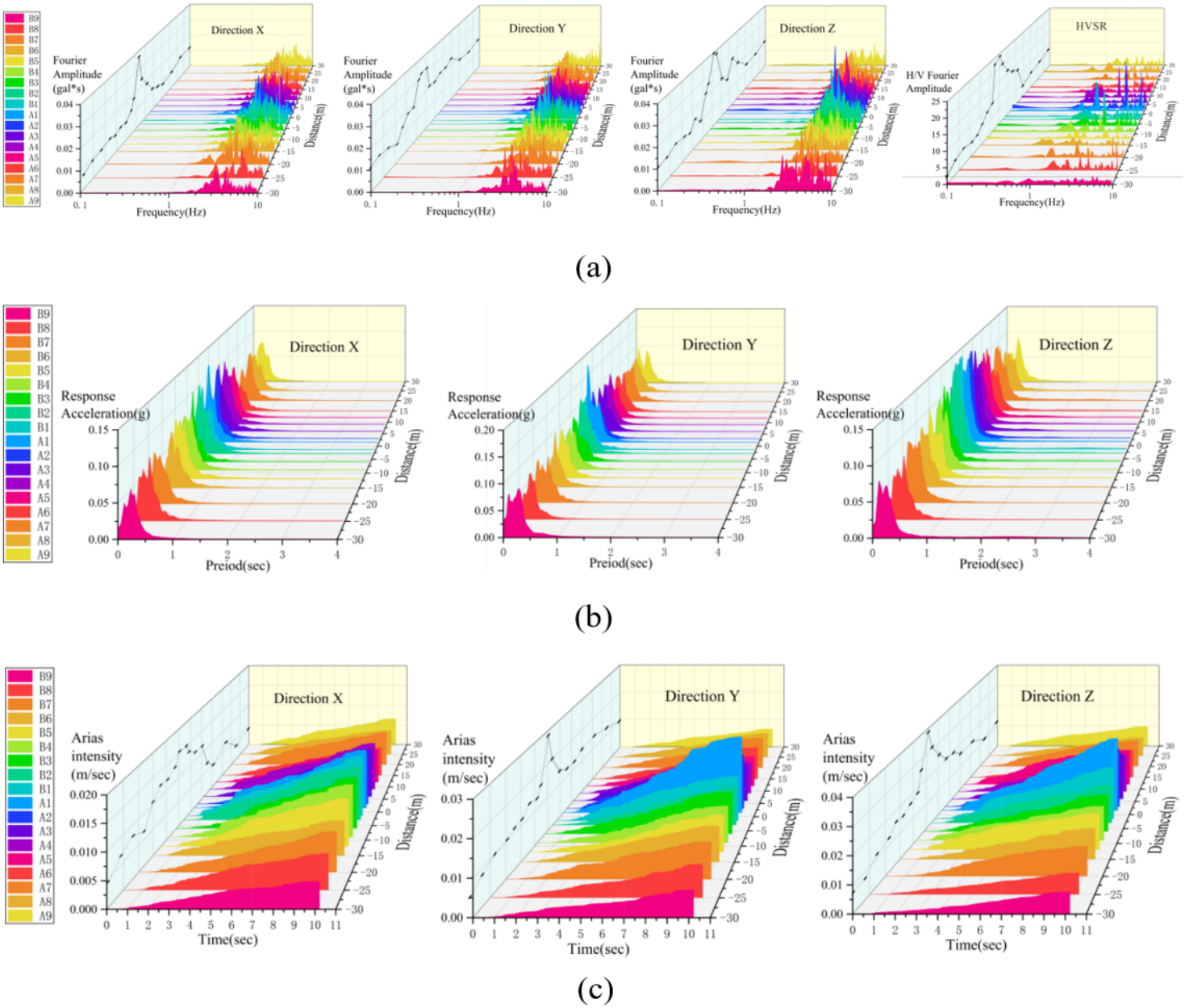

Figure 8

The frequency content of line L5 in Wenshui. a) Fourier amplitude and HVSR, b) Response acceleration, and c) Arias intensity.

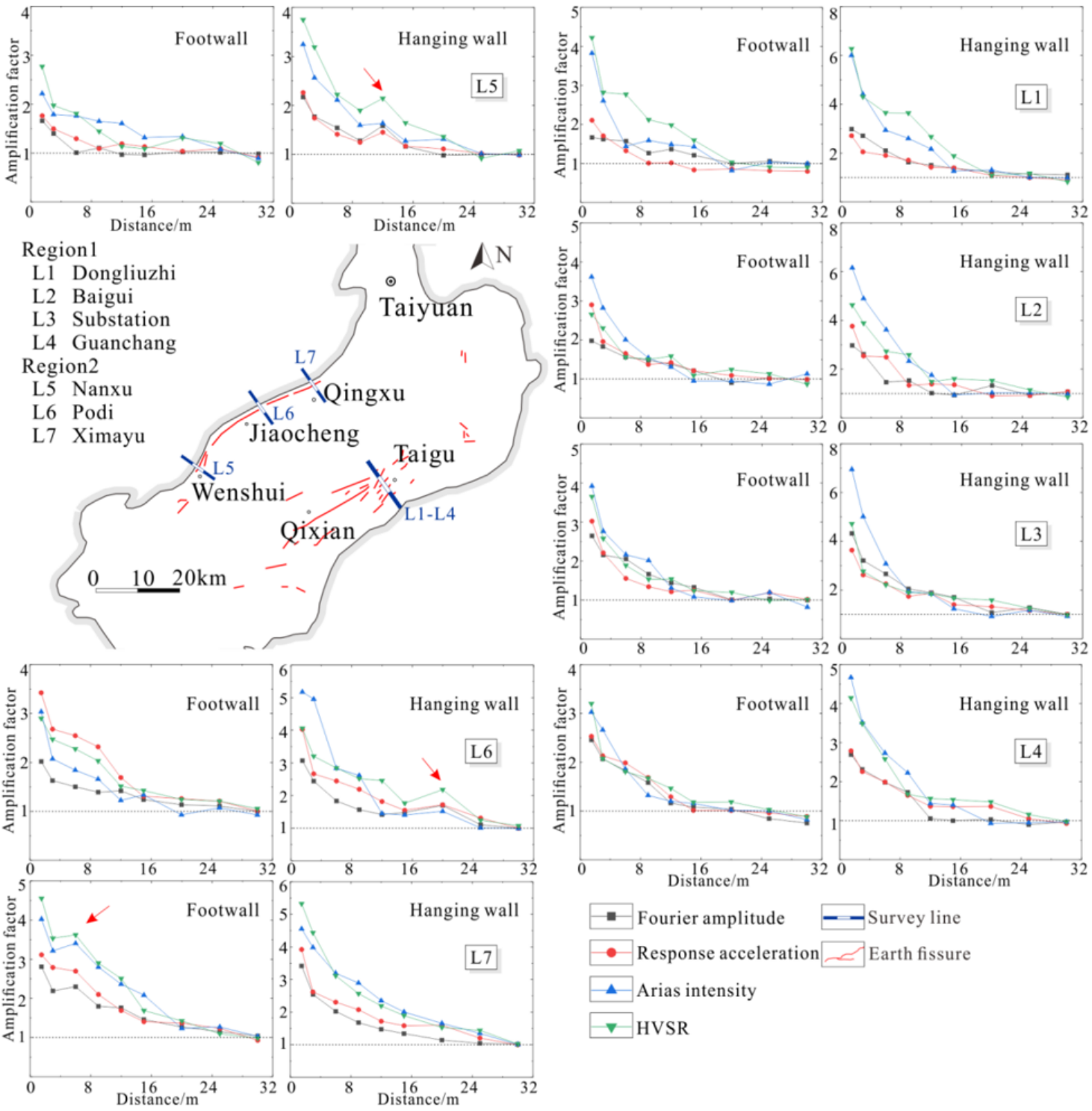

Figure 9

The amplification factor for survey lines L1–L7 Note: The designations employed and the presentation of the material on this map do not imply the expression of any opinion whatsoever on the part of Research Square concerning the legal status of any country, territory, city or area or of its authorities, or concerning the delimitation of its frontiers or boundaries. This map has been provided by the authors.

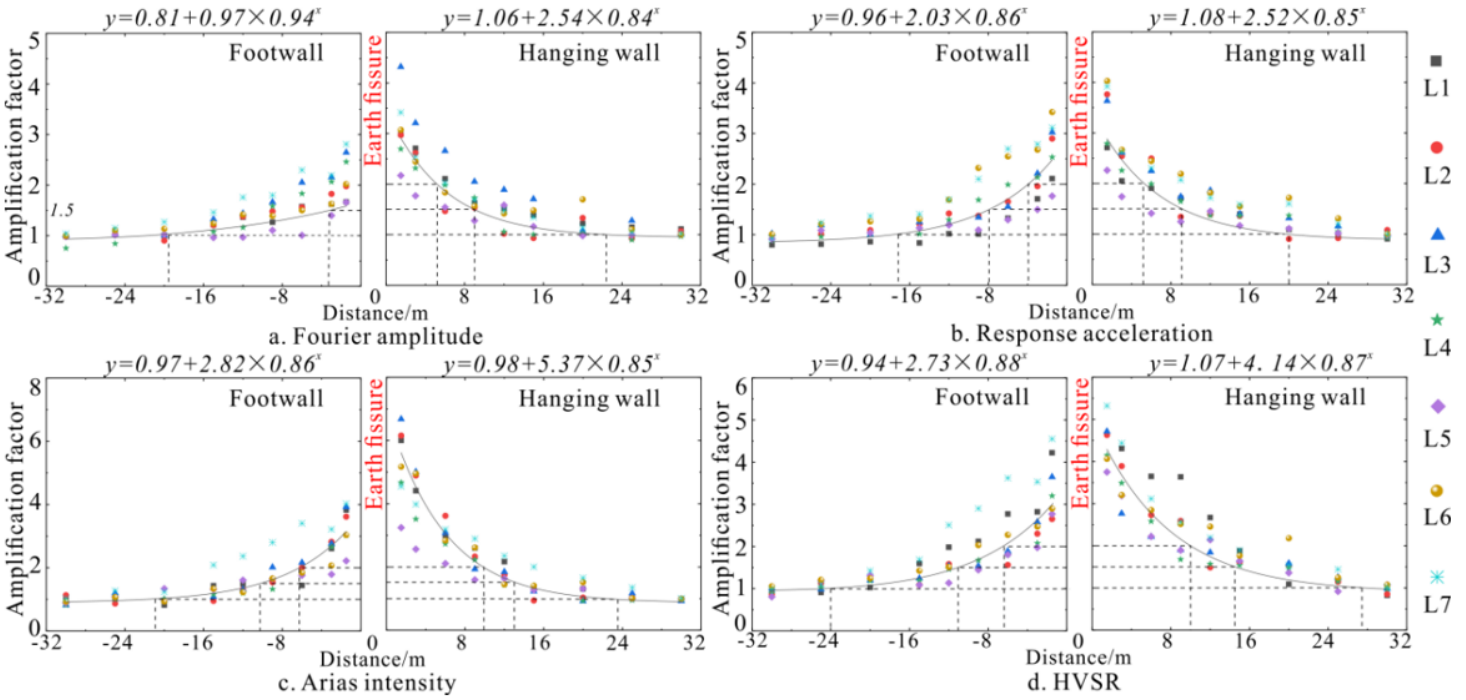

Figure 10

Fitted curves of the amplification factors

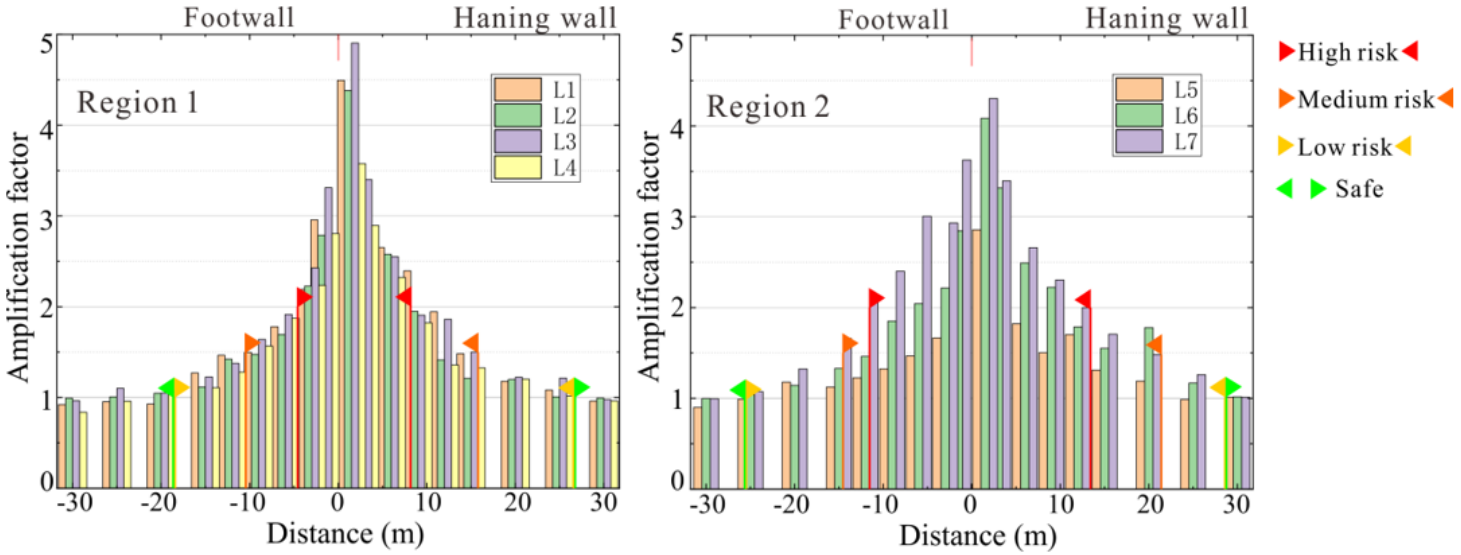

Figure 11

The amplification factors in the different regions